Journal of Power Sources 255 (2014) 219–222

Contents lists available at ScienceDirect

Journal of Power Sources

journal homepage: www.elsevier.com/locate/jpowsour

Short communication

Electrochemical evaluation of carbon nanotubes and carbon black for the cathode of Li–air batteries

Roderick E. Fuentes, Héctor R. Colón-Mercado, Elise B. Fox*

Savannah River National Laboratory, Aiken, SC 29808, USA

HIGHLIGHTS

- Demonstrates the role of carbon on ORR and OER kinetics for Li/air batteries.
- SWCNT had the highest peak current density per gram for ORR and OER.
- SWCNT has a similar onset potential than Au and higher performance.

ARTICLE INFO

Article history:
Received 10 July 2013
Received in revised form
18 December 2013
Accepted 31 December 2013
Available online 8 January 2014

Keywords:
Li/air battery
Cyclic voltammetry
Carbon
Lithium bis(trifluoromethylsulfonyl)imide
Tetraethylene glycol dimethyl ether
Manganese oxide

ABSTRACT

Cyclic Voltammetry (CV) was used to screen carbon catalysts for oxygen reduction reaction (ORR) and oxygen evolution reaction (OER) performance as electrodes for the Li–air battery. Lithium bis(trifluoromethylsulfonyl)imide ($LiTF_2N$) in tetraethylene glycol dimethyl ether (TEGDME) was used as the electrolyte during testing. The effect of manganese/manganese oxide addition on the performance of the carbons was compared to that of the bare carbons in a cycling study. From CV results, it was found that single walled carbon nanotubes (SWCNT) had the highest peak current density per gram for ORR and OER than the other types of carbon studied. The SWCNT ORR peak decreased 49% after 100 cycles and only 36% when manganese/manganese oxide was added. The high activity of SWCNT with manganese/manganese oxide spheres make it a desirable material to use as the cathode for Li–air batteries.

1. Introduction

Electrocatalysts are being considered for the oxygen reduction reaction (ORR) and oxygen evolution reaction (OER) to enhance the discharge/charge reaction kinetics and cyclability for Li–air battery. Several groups working on the electrocatalyst selection have reported similar discharge voltages of a Li–air battery with and without electrocatalysts [1–3], furthermore using carbon by itself has shown to provide high catalytic activity [4–6]. However, most of these studies were performed with organic electrolytes based on carbonates which undergo decomposition and form stable products such as Li_2CO_3 instead of the desired products (i.e., Li_2O_2 and Li_2O) [7,8]. This decomposition contributes to the overpotential of the discharge/charge mechanism, interfering with the validation of new electrocatalyst. There is still a need to find a suitable electrolyte that can be stable during the harsh and oxidizing conditions found in this battery. More recently, ethers such as 1,2-dimethoxyethane (DME) and tetraethylene glycol dimethyl ether (TEGDME) had been considered as stable solvents during oxidative conditions and selectively promote the formation of Li_2O_2 during ORR [9–11].

The inherent complexity of the Li/air battery makes it very difficult to predict and understand catalyst behavior in the cathode. Also, different carbon morphologies can have an effect in performance. For this study, Lithium bis(trifluoromethylsulfonyl)imide ($LiTF_2N$) in TEGDME was used as the electrolyte for comparing the performance of different air electrode materials. TEGDME was selected as the solvent as it has been demonstrated to have high solubility for $LiTF_2N$ and a wide electrochemical window [12]. The different carbon materials were tested for ORR and OER performance using cyclic voltammetry (CV) in a three electrode setup. The experiments seek to evaluate the potentials and reversibility of the reactions occurring at the surface of the air electrode materials without the variables that can affect the performance during full cell assembly testing.

* Corresponding author. Tel.: +1 803 507 8560.
E-mail addresses: ebfox@bellsouth.net, elise.fox@srnl.doe.gov (E.B. Fox).

0378-7753/$ – see front matter © 2014 Elsevier B.V. All rights reserved.
http://dx.doi.org/10.1016/j.jpowsour.2013.12.133

2. Experimental

The materials used were commercially acquired and listed in Table 1. The surface area was obtained utilizing a Micromeritics ASAP2020C, with a 17-point N_2 adsorption–desorption isotherm at 77 K. The $LiTF_2N$ and TEGDME were purchased from 3 M and from Sigma–Aldrich, respectively. Molecular sieves were placed inside the electrolyte solution 24 h prior to use to reduce moisture content. Handling of the electrolyte solution was done inside an Ar filled glovebox. Electrolyte solutions were used when the water content of <100 ppm was achieved. A Karl Fisher Titration was used to determine the moisture content.

Performance for the ORR and OER was obtained using a BASi RDE-2 rotator system enclosed by a plastic glovebox with a continuous flow of dry argon. The system was connected to a computer controlled BASi potentiostat with Epsilon software. The electrodes used consisted of a platinum coil as the counter electrode, a 3 mm diameter disk made of carbon glassy (CG), or gold as the working electrode, and an E-DAQ reversible hydrogen electrode as the reference electrode. The reference potential in the electrolyte solution was 2.72 vs. Li/Li^+ as measure from a Li strip in a solution of 1 M $LiTF_2N$ in TEGDME. Cyclic voltammetry experiments ran between 1.15 and 3.92 V vs. Li/Li^+ for 10 cycles first in a N_2 bubbled solution and then in an O_2 bubbled solution at a scan rate of 100 mV s^{-1}. The data from the N_2 bubbled solution was used to correct for the background current for the performance of during cycling in the O_2 bubbled solution. Carbon inks were prepared with 8 mg of the carbon dispersed in 4 mL of deionized (DI) water and 4 mL of ethanol. For the carbon and manganese containing inks, 4 mg of carbon and 4 mg of QuantumSphere® manganese/manganese oxide were dispersed in 4 mL of DI water and 4 mL of ethanol. A volume of 3.5 μL was placed on top of the working electrode. After it dried at room temperature, 2 μL of a solution of 0.2% w/w of Nafion® in Ethanol was added as a binder. All of the experiments were run at room temperature. The voltammograms presented in Figs. 1 and 2 correspond to a section of the CV. For ORR (Figs. 1(a) and 2(a)) the cathodic scan from 3.5 V to 1.15 V is displayed and for OER (Figs. 1(b) and 2(b)) the anodic scan from 3.5 V to 3.92 V is displayed.

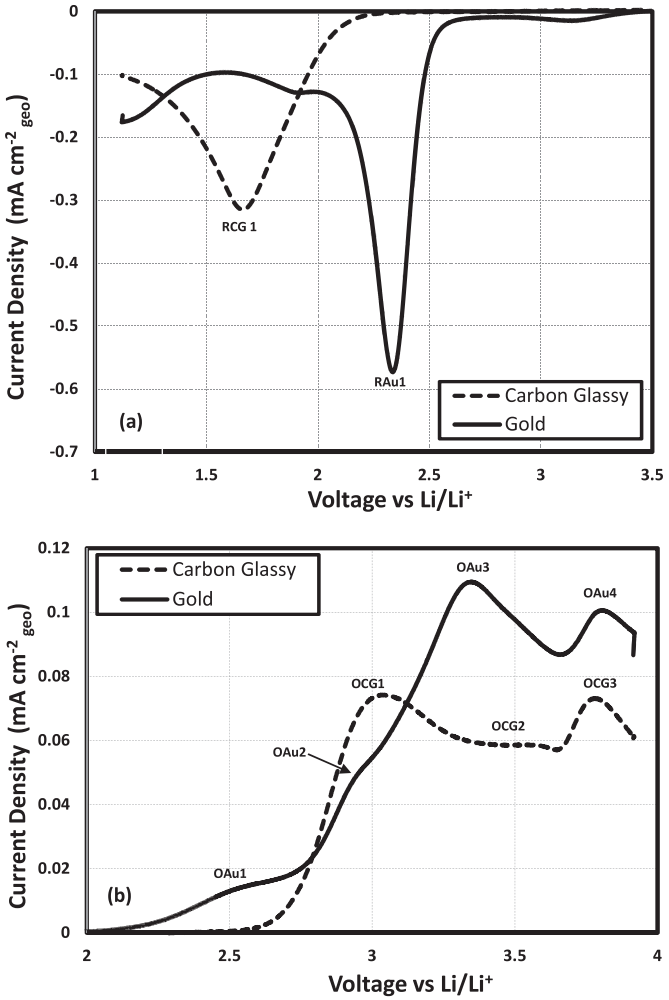

Fig. 1. (a) ORR and (b) OER curves of Carbon Glassy (CG) and Gold (Au) electrode at room temperature.

3. Results and discussion

ORR and OER performance of the electrode itself (without the addition of the carbon inks) in 1 M $LiTF_2N$/TEGDME was first determined by testing electrodes of CG and Au. The potential window during CV was maintained during all experiments to maintain similar peak behavior during OER. It was observed that for OER the shape of the peak can change depending on the selection of a reduction potential limit because as the potential shifts negatively a broad peak can develop in the OER area indicating more than one reduction reaction [10]. Fig. 1 presents the voltammograms of ORR (a) and OER (b) performance while oxygen was being flown in the cell. For ORR a main peak is observed corresponding to reduction peak of CG (RCG1) and reduction peak of Au (RAu1). Compared to CG, Au electrode starts at a lower potential (2.6 V) than CG (2.3 V) for ORR. Additionally the current density is 0.573 mA cm^{-2}_{geo} which is about 45% higher than CG. Therefore, as observed by other researchers Au is more active than CG for ORR [13]. During the oxidation scan, where OER occurs, Au starts at a lower potential than CG, however several oxidation peaks are observed (OAu1, OAu2, OAu3 and OAu4). In the case of CG two main peaks and a broad peak are observed (OCG1, OCG2 and OCG3). These peaks also have less current density than ORR due to insoluble reduction products that can adsorb on the surface of the disk blocking reaction sites. For accounting of the OER, the voltage at ~3.5 V in

Table 1
Physical properties of the different materials tested.

Carbon material	BET surface area (m^2 g^{-1})	Pore volume (cm^3 g^{-1})	Particle size[b]
Carbon black (Vulcan XC-72R, Cabot, Inc.)	220	0.35	27 nm[a]
Carbon black (Ketjenblack EC600JD, Akzo Nobel)	1410	2.72	4 nm[a]
Carbon nanofiber (PR-19-XT-HHT, Pyrograf III)	8	0.05	150 nm * 50–200 μm
Single-wall carbon nanotubes (Bucky USA)	1115	0.98	0.7–2.5 nm * 0.5–10 μm
Multi-wall carbon nanotubes (Sigma–Aldrich)	299	0.88	20–25 nm * 1–5 μm
Manganese/manganese oxide QSI-Nano® (QuantumSphere)	26	0.14	30–50 nm

[a] As determined by BET.
[b] Particle size as reported by manufacturer unless otherwise noted.

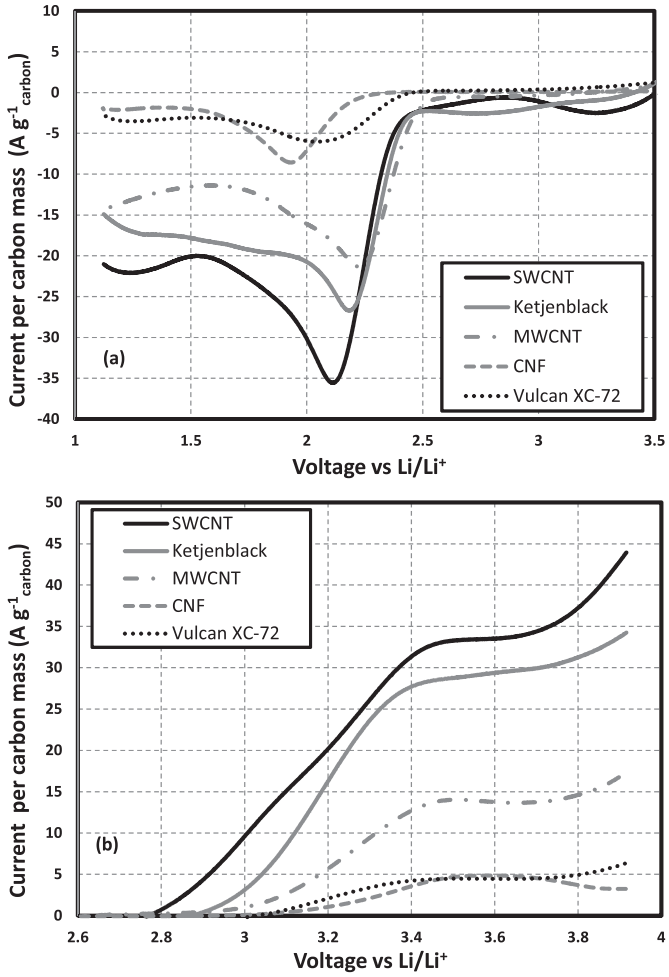

Fig. 2. (a) ORR and (b) OER curves of several carbon materials obtained at room temperature.

TEGDME was found to be the main peak obtained during oxidation [14]. The several peaks found in Au and CG are related to the oxidation reactions of lithium oxides and can occur due to the selection of a low cathodic potential (1.15 V) [10]. The highest current density was for peak OAu3 for gold and OCG1 for CG. Although, gold has a higher current density, CG peak appeared at a lower potential. For OER CG has higher performance than Au.

The results for ORR are complementary to a previous electrode study by Lu et al. [15] in $LiClO_4$/DME, which found that the activity of the series to be Au > CG and in correlation of oxygen adsorption energy, but also highlight the impact of electrolyte selection when examining electrode performance. Unsupported Au has previously been used to demonstrate the reversibility of the $Li-O_2$ battery at a high rate [16], however conflicting results have also shown that supported Au on carbon is relatively inactive for Li_2O_2 oxidation [17]. In the case of GC the activity for both ORR and OER is relatively high, making it a suitable electrode material. Recently published results using the same electrolyte show CG under cycling conditions. The current density results for ORR and OER was reduced to almost zero at only 30 cycles [18]. Other carbon materials with high surface area and distinct morphologies were considered as electrodes to provide more stability during cycling.

The effect of different carbons on the cycle performance of the CG electrode was also studied. The physical properties of the different carbon materials are shown in Table 1. It is observed that the highest surface area materials are Ketjenblack and single-wall carbon nanotubes (SWCNT) in which surface areas surpass 1000 $m^2\ g^{-1}$. In addition, Ketjenblack has a very high pore volume compared to the other carbon materials studied. All materials were tested for ORR and OER and the results of the CV are presented in Fig. 2. For ORR, the material with the lowest onset potential is carbon nanofiber (CNF) followed by Vulcan, while SWCNT, MWCNT and Ketjenblack have the highest onset potentials. CNF and Vulcan have similar peak current density, even though the surface area of CNF is 96% lower than the surface area of Vulcan, the graphitic nanostructure of the carbon fibers can contribute in the performance of ORR. Similar activity behavior was obtained for OER for the carbon materials in which carbon Ketjenblack and SWCNT have the highest activity. Although, Vulcan was used in a previous publication to help in the OER at voltages more than 4 V, at the lower voltages studied it did not seen to help compared to the other carbons studied [17]. SWCNT had the highest current per gram for ORR and OER of all the materials studied. The results indicate that there appears to be a link between high surface area and 1D graphitic-nanostructure that can be very advantageous for the reduction/oxidation of the lithium oxides. In addition, the onset potential for ORR of this material is similar to Au (Fig. 1), which reiterates the importance of carbon and its structure to attain high performance.

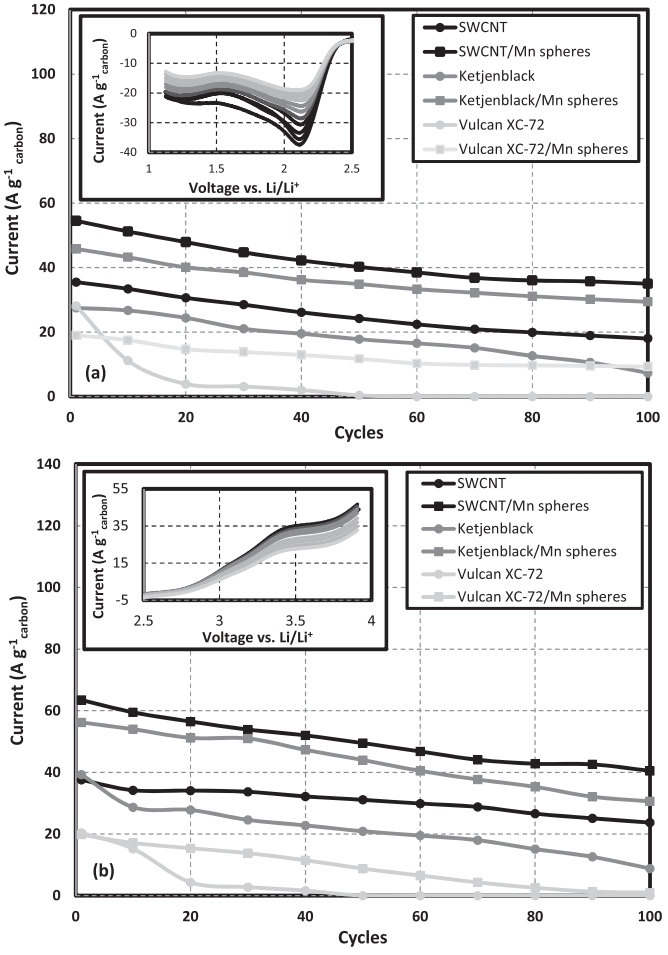

Fig. 3. (a) ORR and (b) OER peak current per gram of carbon during cycling for single wall carbon nanotubes, Vulcan and Ketjenblack. The different types of carbon were mixed 1:1 with manganese/manganese oxide (Mn spheres) and the corresponding results are also shown. In the insert of (a) is presented SWCNT linear voltammetries at low potentials. In the insert of (b) is presented SWCNT linear voltammetries at high potentials.

Potential cycling was used to assess the performance of the carbon materials during continuous discharge/charge. Fig. 3 shows the performance of the two highest performing materials (SWCNT and Ketjenblack) compared with Vulcan during 100 cycles for ORR (a) and OER (b). The results seek to elucidate the effects of cycling on the carbon and the synergetic effects of adding manganese/manganese oxide (abbreviated to Mn spheres in Fig. 3) catalyst in a 1:1 weight mixture. Manganese/manganese oxide was selected as it is among the proposed electrocatalysts for the lithium-air battery and has been used in several publications [1,12,19–21]. All the tested samples show the peak current decreases as a function of cycling. The ORR current degrades linearly except for Vulcan where the carbon deactivates after 20 cycles. The addition of manganese oxide to the carbons has a positive effect, maintaining the peak current at longer cycles than bare carbons. This behavior is believed to be caused by manganese oxide which improves capacity of the charge/discharge cycle [1,3,12,22]. In the case of Vulcan, manganese/manganese oxide allows stable performance during the test, even though Vulcan started at an initial current 51% higher than with the addition of manganese oxide for ORR. After 10 cycles the performance is highest for SWNT/Mn spheres > Ketjenblack/Mn spheres > SWNT > Ketjenblack > Vulcan/Mn spheres > Vulcan. The behavior of the electrocatalysts for the OER is similar to the ORR, where manganese oxide allows for higher peak current densities and maintain stability of each carbon during ORR. A visible difference between the OER and ORR performance can be seen with the carbon blacks (Vulcan and Ketjenblack). While Ketjenblack shows stable performance during the ORR, in the OER Ketjenblack's performance decreases exponentially after 70 cycles. This exponential decrease was also seen in Vulcan after only 10 cycles, however it is seem that is characteristic of the carbon black studied because it is not observed in SWCNT performance. Comparing these materials during cycling a similar conclusion it is observed that nanostructure form is important to maintain cyclability. Also it is observed that the addition of manganese oxide to all the carbons can extend peak current density during ORR.

4. Conclusion

With the use of the three electrode setup, ORR and OER performance was obtained for several common carbon materials with different physical properties and structures. A comparison between different carbon allotropes showed different stability performance. It is observed that SWCNT has the highest performance for ORR and OER and the onset potential for ORR is similar to Au. The SWCNT ORR peak decreased 49% after 100 cycles and only 36% when manganese/manganese oxide was added. The high activity of SWCNT with manganese/manganese oxide spheres make it a desirable material to use as the cathode for Li–air batteries. Manganese/manganese oxide was found to enhance the stability SWCNT and carbon blacks during ORR, while no major effect was found for OER (except for Ketjenblack).

Acknowledgments

This project was funded by SRNL LDRD Programs and DOE Vehicle Technologies. Savannah River National Laboratory is operated by Savannah River Nuclear Solutions. This document was prepared in conjunction with work accomplished under Contract No. DE-AC09-08SR22470 with the U.S. Department of Energy.

References

[1] A. Débart, A.J. Paterson, J. Bao, P.G. Bruce, Angew. Chem. Int. Ed. 47 (2008) 4521–4524.
[2] J. Read, J. Electrochem. Soc. 149 (2002) A1190–A1195.
[3] G.Q. Zhang, J.P. Zheng, R. Liang, C. Zhang, B. Wang, M. Au, M. Hendrickson, E.J. Plichta, J. Electrochem. Soc. 158 (2011) A822–A827.
[4] E. Yoo, H. Zhou, ACS Nano 5 (2011) 3020–3026.
[5] B. Sun, B. Wang, D. Su, L. Xiao, H. Ahn, G. Wang, Carbon 50 (2012) 727–733.
[6] Y. Yang, Q. Sun, Y.-S. Li, H. Li, Z.-W. Fu, J. Electrochem. Soc. 158 (2011) B1211–B1216.
[7] B.D. McCloskey, D.S. Bethune, R.M. Shelby, G. Girishkumar, A.C. Luntz, J. Phys. Chem. Lett. 2 (2011) 1161–1166.
[8] W. Xu, J. Hu, M.H. Engelhard, S.A. Towne, J.S. Hardy, J. Xiao, J. Feng, M.Y. Hu, J. Zhang, F. Ding, M.E. Gross, J.-G. Zhang, J. Power Sources 215 (2012) 240–247.
[9] J. Wu, H.W. Park, A. Yu, D. Higgins, Z. Chen, J. Phys. Chem. C 116 (17) (2012) 9427–9432.
[10] C.O. Laoire, S. Mukerjee, K.M. Abraham, E.J. Plichta, M.A. Hendrickson, J. Phys. Chem. C 114 (2010) 9178–9186.
[11] C.O. Laoire, S. Mukerjee, E.J. Plichta, M.A. Hendrickson, K.M. Abraham, J. Electrochem. Soc. 158 (2011) A302–A308.
[12] O. Oloniyo, S. Kumar, K. Scott, J. Electron. Mater. 41 (2012) 921–927.
[13] Y.-C. Lu, H.A. Gasteiger, E. Crumlin, J.R. McGuire, Y. Shao-Horn, J. Electrochem. Soc. 157 (2010) A1016–A1025.
[14] M.J. Trahan, S. Mukerjee, E.J. Plichta, M.A. Hendrickson, K.M. Abraham, J. Electrochem. Soc. 160 (2013) A259–A267.
[15] Y.-C. Lu, H.A. Gasteiger, Y. Shao-Horn, J. Am. Chem. Soc. 133 (2011) 19048–19051.
[16] Z. Peng, S.A. Freunberger, Y. Chen, P.G. Bruce, Science (Washington, DC, U.S.) 337 (2012) 563–566.
[17] J.R. Harding, Y.-C. Lu, Y. Tsukada, S.-H. Yang, Phys. Chem. Chem. Phys. 14 (2012) 10540–10546.
[18] R. Tatara, N. Tachikawa, H.M. Kwon, K. Ueno, K. Dokko, M. Watanabe, Chem. Lett. 42 (2013) 1053–1055.
[19] T.T. Truong, Y. Liu, Y. Ren, L. Trahey, Y. Sun, ACS Nano 6 (2012) 8067–8077.
[20] A.K. Thapa, T. Ishihara, J. Power Sources 196 (2011) 7016–7020.
[21] H. Cheng, K. Scott, J. Power Sources 195 (2010) 1370–1374.
[22] E.M. Benbow, S.P. Kelly, L. Zhao, J.W. Reutenauer, S.L. Suib, J. Phys. Chem. C. 115 (2011) 22009–22017.